AIP | Journal of Applied Physics

Reuse of GaAs substrates for epitaxial lift-off by employing protection layers

Kyusang Lee, Jeramy D. Zimmerman, Xin Xiao, Kai Sun, and Stephen R. Forrest

Citation: J. Appl. Phys. **111**, 033527 (2012); doi: 10.1063/1.3684555

View online: http://dx.doi.org/10.1063/1.3684555

View Table of Contents: http://jap.aip.org/resource/1/JAPIAU/v111/i3

Published by the American Institute of Physics.

JOURNAL OF APPLIED PHYSICS **111**, 033527 (2012)

Reuse of GaAs substrates for epitaxial lift-off by employing protection layers

Kyusang Lee,[1] Jeramy D. Zimmerman,[1] Xin Xiao,[1] Kai Sun,[2] and Stephen R. Forrest[1,2,3,a)]
[1]*Department of Electrical Engineering and Computer Science, University of Michigan, Ann Arbor, Michigan 48109, USA*
[2]*Department of Material Science and Engineering, University of Michigan, Ann Arbor, Michigan 48109, USA*
[3]*Department of Physics, University of Michigan, Ann Arbor, Michigan 48109, USA*

(Received 19 October 2011; accepted 18 January 2012; published online 15 February 2012)

We demonstrate repeated use of GaAs wafers for multiple growths by employing lattice-matched epitaxial protection layers to preserve the wafer surface in its original condition following their etch removal after growth. The protection layers provide a regrowth surface that eliminates the need for repolishing prior to subsequent growth. Between growths, the protection layers are removed by wet chemical etching. The resulting surface quality is examined using atomic force microscope and energy dispersive spectrometry. We show that the surface roughness, chemical composition, morphology, and electronic properties of the GaAs surface after protection-layer removal are comparable to that of the original substrate surface. We show that *p-n* junction GaAs solar cells grown on original and reused wafers have nearly identical performance with power conversion efficiencies of ∼23%, under simulated 1 sun illumination, AM1.5 G. The high power conversion efficiency of GaAs solar cells combined with reduced costs associated with multiple parent wafer reuses promise cost competitiveness with incumbent solar cell technologies. *© 2012 American Institute of Physics*. [doi:10.1063/1.3684555]

I. INTRODUCTION

GaAs-based epitaxial lift-off (ELO) solar cells exhibit superior power conversion efficiency compared with alternative single-junction photovoltaic cell designs, such as those based on crystalline Si, copper indium gallium sulfide (CIGS), CdTe, and even comparable GaAs cells left on their growth substrates.[1,2] The ELO process enables the bonding of thin, single-crystal III-V active layers onto secondary substrates (e.g., plastic) that are both lightweight and flexible.[3–7] A lifted-off solar cell with a reflective back contact requires approximately half of the active region thickness to absorb an equivalent amount of incident radiation compared to conventional substrate-based solar cells, reducing materials consumption and growth time of the epitaxial layers.[8,9] Miller *et al*. reported that the reflective back contact enables photon recycling by light trapping while also concentrating the carriers in a thin layer that leads to an increased open circuit voltage compared with equivalent, substrate-based solar cells.[10] Among these benefits, the major advantage is the potential for wafer reuse following ELO of the solar cell active region, which can enable significant manufacturing cost reductions by minimizing the consumption of expensive wafers.[3,11] Indeed, wafer reuse has recently been demonstrated for InP-based solar cells. We extend this previous work to investigate the feasibility of GaAs wafer reuse following lift-off by employing a combination of epitaxial protection layers and materials etchants to preserve the wafer surface for subsequent epitaxial layer growth.

It is widely observed that the conventional ELO process results in significant wafer surface roughening and accumulation of contaminants.[3,11] To eliminate these defects in preparation for subsequent epitaxial growth, a polishing etch process is typically employed. However, this process does not generally provide a high quality regrowth interface; thus device layers grown on a chemically polished surface after ELO results in dramatic performance degradation of subsequently fabricated solar cells.[11] To ameliorate this problem, chemo-mechanical wafer repolishing is required; however, this consumes tens of microns of material from the top surface of the wafer while often inflicting additional surface and edge damage, thereby limiting the potential number of wafer reuses.

Here, we employ lattice-matched epitaxial protection layers to preserve the original GaAs wafer surface in its epi-ready condition, thereby providing a high-quality regrowth interface without polishing. The methods used are analogous to those reported for InP wafer reuse.[3] In this case, however, we employed $In_{0.49}Ga_{0.51}P$ as a surface protection layer to provide an As-free surface adjacent to the AlAs sacrificial layer that is ultimately removed via a material-selective etchant (hydrofluoric acid) to part the epitaxy from the substrate. Since Al-free III-V alloys are also etched slowly in HF, the protection layer surface is damaged. Therefore, an $In_{0.49}Ga_{0.51}P/GaAs/In_{0.49}Ga_{0.51}P$ lattice-matched protection layer system is employed. The InGaP layer adjacent to the AlAs protects the GaAs layer from HF, and then selective removal of GaAs and the other InGaP layers provides the required high quality, epi-ready growth interface. The sequential removal of the three protection layers assists in removing surface residues and particulates that cannot be eliminated with only a single protection layer etch.

We test the ELO protection layer sequence and removal processes by exposing the protected wafer to an HF-based solution for extended periods. The morphology and chemistry of the surface of the original wafer, and that of the wafer after

---

[a)] Author to whom correspondence should be addressed. Electronic mail: stevefor@umich.edu.

protection layer removal (referred to as the surface-protected wafer) are found to be nearly identical. Furthermore, the properties of the GaAs solar cells fabricated on layers grown on both wafer sets, have similar power conversion efficiencies of approximately 23%. Optical and materials analysis of the original and regrown layers also indicate little or no change between growths. The high power conversion efficiency of GaAs solar cells combined with multiple reuses of the parent wafer promise cost-competitiveness with other photovoltaic materials systems, such as Si, CIGS, and CdTe.

This paper is organized as follows: in Sec. II we give details of our experimental methods, in Sec. III our results and discussion of the initial and subsequent epitaxial layer growths are provided, and in Sec. IV we provide conclusions.

II. EXPERIMENTAL

The layer structures were grown by gas-source molecular beam epitaxy (GSMBE) on Zn-doped, (100) p-GaAs substrates. All growths started with a 0.2 μm thick 2×10^{18} cm^{-3} Be-doped GaAs buffer layer. For the reference photovoltaic cells, the layer structure is as follows (see Fig. 1(a)): 0.2 μm thick, 2×10^{18} cm^{-3} Be-doped GaAs buffer layer, 75 nm thick, 4×10^{17} cm^{-3} Be-doped $In_{0.49}Ga_{0.51}P$ back-surface field (BSF) layer, 3.5 μm thick, 2×10^{17} cm^{-3} Be-doped p-GaAs base layer, 0.15 μm thick, 1×10^{18} cm^{-3} Si-doped n-GaAs emitter layer, 25 nm thick, 2×10^{18} cm^{-3} Si-doped $Al_{0.5}In_{0.5}P$ window layer, and a 0.2 μm thick, 5×10^{18} cm^{-3} Si-doped n-GaAs ohmic contact layer. The protection trilayer consists of 0.1 μm thick, $In_{0.49}Ga_{0.51}P$, 0.1 μm thick GaAs layer, and a second 0.1 μm thick $In_{0.49}Ga_{0.51}P$ layer. All protection layers are undoped. To simulate the epitaxial lift-off process, samples with protection and 60 nm thick undoped AlAs sacrificial layers (Fig. 1(b)) are then exposed to a 7.5% HF : H_2O solution for 48 h. After epitaxial layer removal, the $In_{0.49}Ga_{0.51}P$ and GaAs protection layers are selectively removed by etching in H_3PO_4 : HCl (1 : 1) for 1 min, followed by H_3PO_4 : H_2O_2 : H_2O (3 : 1 : 25) for 30 s. Subsequently, etching in H_3PO_4 : HCl : H_2O (1 : 1 : 1) and then HCl : H_2O (1 : 1) for 1 min each removes the final $In_{0.49}Ga_{0.51}P$ protection layer. The substrate is loaded back into the GSMBE chamber and degassed. A second or third sample cell is then grown on the original parent substrate with structures identical to that of the reference device.

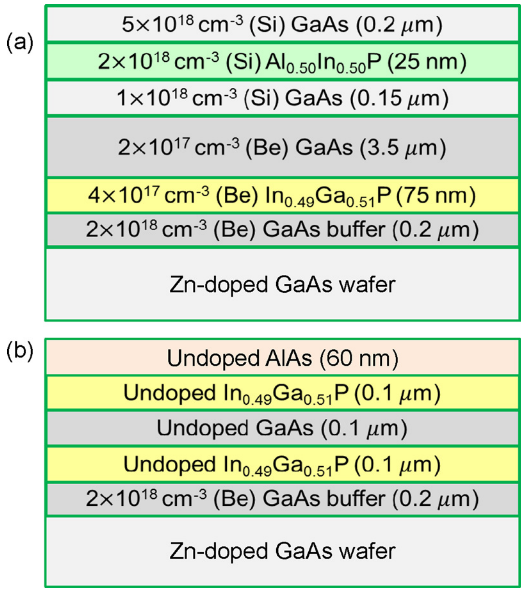

FIG. 1. (Color online) Schematic diagram of (a) the GaAs solar cell layer structure, and (b) the trilayer epitaxial protection scheme including the AlAs sacrificial layer.

After photolithographically defining 5 × 5 mm mesas, a 4 μm deep wet etch of the epitaxial layers in H_3PO_4 : H_2O_2 : H_2O (3 : 1 : 25) for 11 min was followed by 1 min in H_3PO_4 : HCl (1 : 1). Then, a Ni (5 nm)/Ge (32 nm)/Au (65 nm)/Ti (20 nm)/Au (1000 nm) n-type contact metal grid was deposited using e-beam evaporation, photolithographically defined, followed by photoresist lift-off. The aperture of the metal grid with 75 μm wide bus bars and 3 μm wide fingers was 94%. The p-type contact consisting of Pd (5 nm)/Zn (20 nm)/Pd (20 nm)/Au (1000 nm) was next deposited on the reverse side of the wafer. For ohmic contact formation, both metal alloys were rapidly annealed at 410 °C for 60 s followed by contact layer removal by BCl_3 and Ar-based chemically assisted physical plasma etching. Finally, a ZnS/MgF_2 bilayer was deposited on the top surface to minimize optical reflections.

To assess the material quality, Hall-effect measurements were made on 1 μm thick, Si-doped GaAs layers grown on both the original and used wafer surfaces following epitaxial and protection layer removal. For cross-sectional scanning transmission electron microscopy (STEM) images obtained

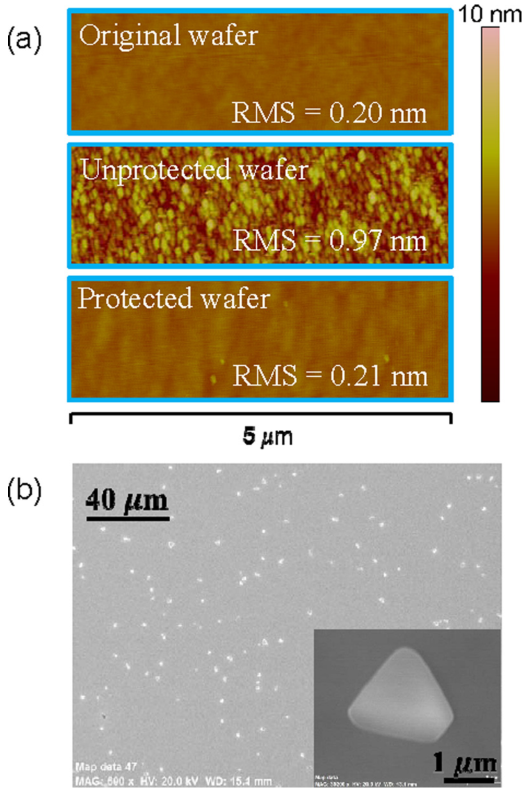

FIG. 2. (Color online) AFM images of the original epi-ready GaAs substrate surface, HF exposed GaAs substrate surface after the epitaxial growth, and removal of protection layers, and the surface without a protection layer. (b) SEM image of an HF exposed wafer surface without protection layers.

with a JOEL 2100 F TEM with a probe corrector in the high-angle annular dark-field imaging mode, 0.5 μm thick, undoped GaAs layers were grown on both original, first, and second epitaxies. A 1 μm thick, undoped $GaAs/Al_{0.7}Ga_{0.3}As$ double heterostructure was grown for photoluminescence measurements on both the original and used wafers. Furthermore, to investigate the effectiveness of the protection layer scheme in preventing surface damage, a 0.2 μm thick GaAs buffer layer was grown on an original wafer without a protection layer, and was then examined as described above. The morphology and chemical composition of the surfaces of the original, surface-protected and unprotected wafers were compared using atomic force microscopy (AFM), scanning electron microscopy (SEM), three-dimensional laser microscopy, energy dispersive spectrometry (EDS), and x-ray photoelectron spectrometry (XPS).

III. RESULTS AND DISCUSSION

To use the same wafer for multiple growths, it is essential to preserve the original surface morphology and chemistry at all steps throughout the process. The AFM images (Fig. 2(a)) show a root-mean-square roughness of $RMS = 0.20$ nm for the original wafer surface, $RMS = 0.97$ nm after ELO on the unprotected surface, and $RMS = 0.21$ nm for the surface after the $In_{0.49}Ga_{0.51}P/GaAs/In_{0.49}Ga_{0.51}P$ trilayer was removed from the protected substrate. The surface roughness of GaAs exposed directly to dilute HF increases fivefold from that of the original wafer, whereas the protected wafer shows no change. Additionally, three-dimensional laser microscopy and surface profile measurements (not shown) over larger areas (128×128 μm and 3×3 mm, respectively) indicate that the RMS surface roughness is > 20 nm for the unprotected wafer, which is two orders of magnitude larger than the original wafer due to the formation of a high concentration of micron size particles over the wafer surface. Figure 2(b) shows these particles as observed by SEM. The rough, particle-covered surface prevents the subsequent growth of layers of the same quality as on the original surface, and eventually results in the degradation of regrown photovoltaic device performance.[11] In contrast, the pristine condition of the protected substrate after layer removal suggests the feasibility of wafer reuse. Moreover, protection layer removal does not consume the original wafer material; hence, the number of wafer reuses is potentially unlimited.

To compare the surface chemistry and effectiveness of protection layers on exposure to etchants with that of the as-grown surface, EDS data for the surfaces of fresh, unprotected, and protected wafers were obtained. Figure 3 shows EDS maps of O, Ga, and As for the surfaces of the three different samples. Original and surface-protected wafers show nearly identical chemical compositions, whereas surfaces exposed to HF while lacking a protection layer exhibit locally concentrated oxygen with a corresponding deficiency of elemental Ga. The shape of the oxidized feature is consistent with the presence of a micron-scale particle as shown in Fig. 2(b), inset. This suggests the formation of As_2O_5 on the surface during the etch process.

Figure 4 shows the EDS data for the same samples as in Fig. 3. The concentrations of O extracted from the spectra for

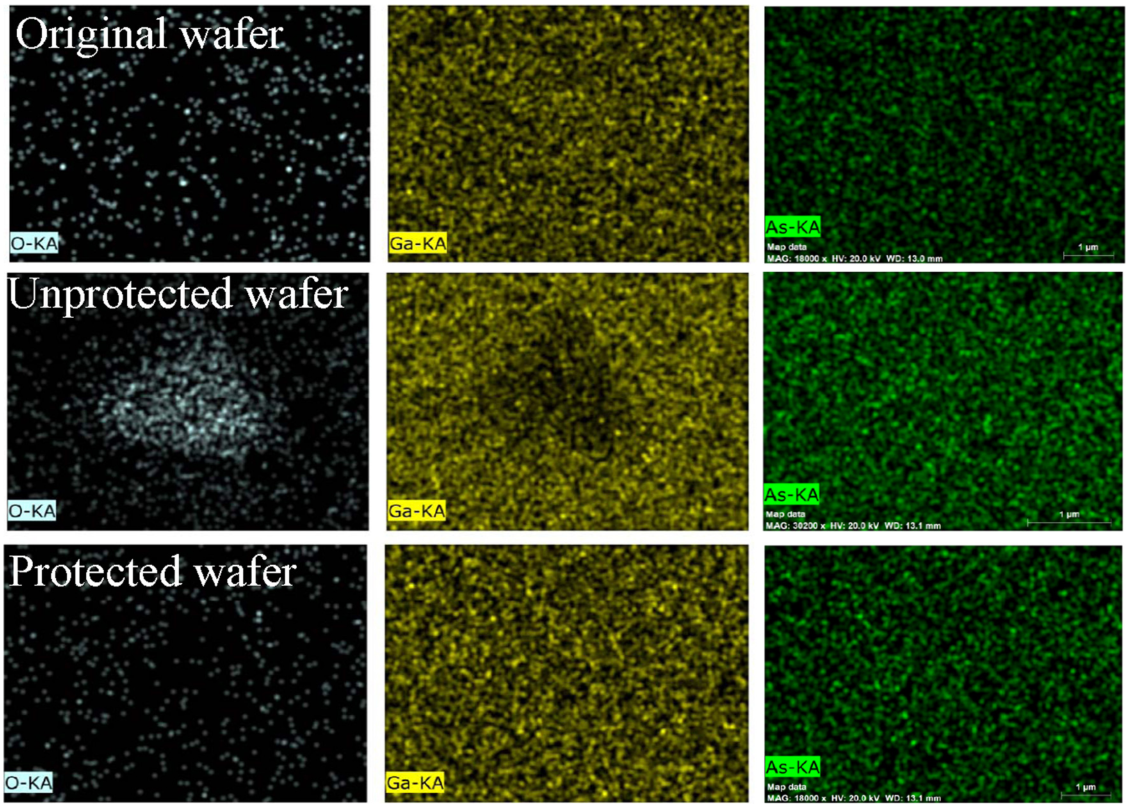

FIG. 3. (Color online) Hybrid mapping of elemental oxygen, gallium, arsenic near the surface of original, surface protected, and unprotected wafers after the protection layers were removed. The elemental compositions are shown in each image.

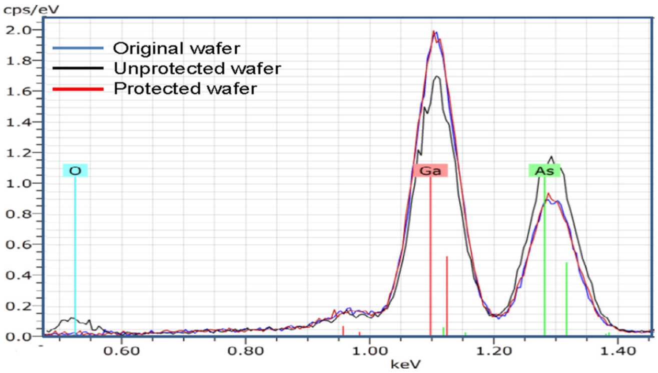

FIG. 4. (Color online) Energy dispersive spectra of wafers in Fig. 2.

the original, protected and unprotected wafers over the surface were 2.2%, 0.7%, and 25.6%, respectively. Also, the atomic ratios of Ga to As were 48.3% : 49.5%, 49.5% : 50.3%, and 33.2% : 41.2% with ±0.4% error, respectively. The fresh and protected samples show similar Ga : As ratios with low oxygen concentration. Using P-based protection layers, the formation of As_2O_5 on the surface during etching is prevented, which is not the case when using As-containing layers. This conclusion is supported by the XPS data in Fig. 5. Original and protected wafer surfaces exhibit nearly identical As and As_2O_5 peak intensities at 41 eV and 45 eV, respectively, however, the unprotected surface shows a weak As and strong As_2O_5 peak intensity. Moreover, the XPS measurements (not shown) indicate a negligible difference between original and regrown wafer surfaces following protection layer removal without the appearance of additional peaks, indicative of a chemically unchanged surface before and after protection layer removal and regrowth.

Figure 6 shows cross-sectional, high angle annular dark field images of an undoped GaAs layer at the growth interface. The reference epitaxial layer was grown on the original, epi-ready wafer, and identical structures were grown on protected and etched wafer surfaces that have been exposed to this cycle twice, with the surface protection layers removed following each growth sequence. The cross-sectional, atomic resolution STEM image shows the nearly perfect crystalline growth without any apparent defects for all samples. This indicates that the quality at the growth interface after protection layer removal is unchanged from that of the original wafer.

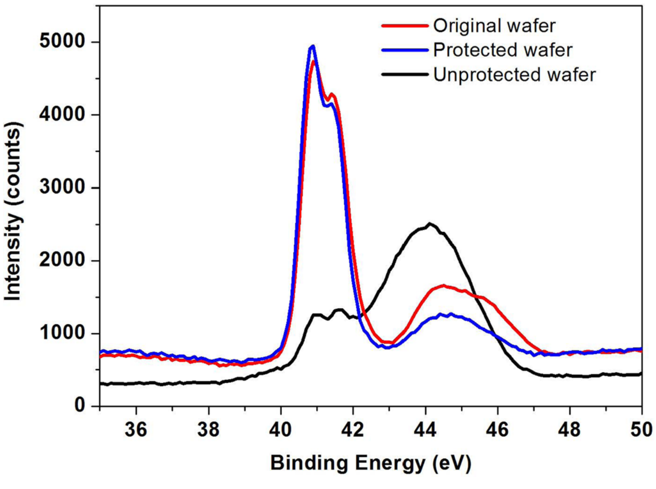

FIG. 5. (Color online) X-ray photoelectron emission spectra of the samples in Fig. 2.

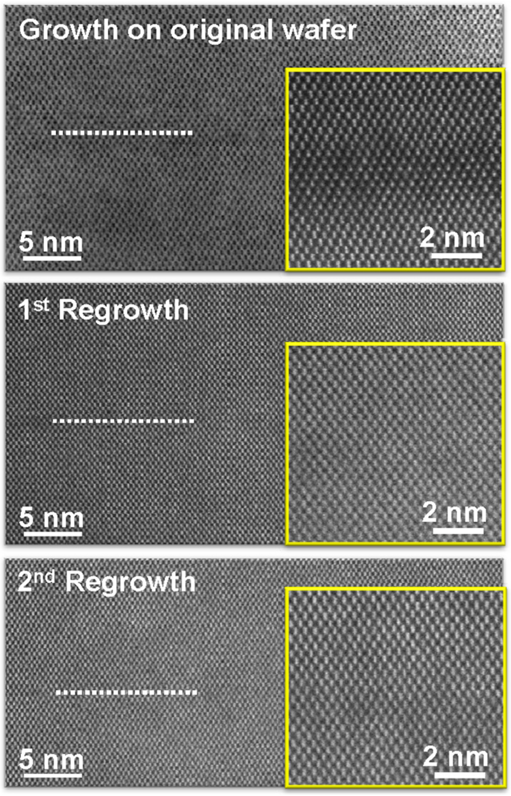

FIG. 6. (Color online) Atomic resolution cross-sectional transmission electron microscope images of the growth interface between the wafer and epitaxial GaAs layer grown on (a) original, (b) first epitaxial, and (c) second epitaxial growth steps. Dotted lines indicate the starting growth interfaces. Insets show details of the growth interfaces.

The Hall effect doping concentrations of the Si-doped, 1 μm thick GaAs layers of the original and regrown samples were $(1.62 \pm 0.05) \times 10^{18}$ cm^{-3} and $(1.66 \pm 0.12) \times 10^{18}$ cm^{-3}, respectively, and the Hall mobilities were 2030 ± 80 cm^2/V s and 2050 ± 120 cm^2/V s, respectively. The small differences between samples are due to run-to-run variations.

Photoluminescence (PL) spectra of the samples were compared using a 20 mW, $\lambda = 473$ nm wavelength diode pump laser. Figure 7 shows the PL intensity between $\lambda = 820$ nm and $\lambda = 900$ nm for three samples consisting of a 0.1 μm thick undoped $Al_{0.7}Ga_{0.3}As$, a 1μm thick undoped GaAs, and a 0.1 μm thick undoped $Al_{0.7}Ga_{0.3}As$ double heterostructure grown on an original (reference), protected and unprotected wafer. The data indicate that losses due to nonradiative recombination are comparable between the layers grown on the fresh and used protected wafer. However, the weak PL intensity of the structure grown on the unprotected substrate is further evidence of a degraded surface. The inset provides the reflection high energy electron diffraction (RHEED) patterns obtained from the wafer surface in the GSMBE chamber. The original wafer clearly exhibits a 2×4 reconstruction after 100 monolayers of buffer layer growth. The nearly identical streak pattern after ~100 monolayers of growth after epitaxial protection layer removal indicates that the surface roughness is unchanged from that of

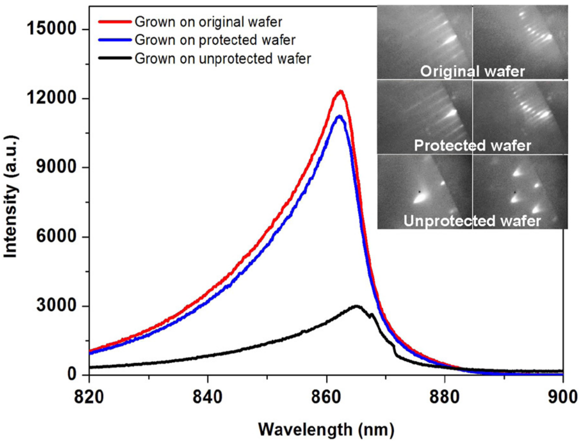

FIG. 7. (Color online) Photoluminescence spectra at room temperature (300 K) from an $Al_{0.7}Ga_{0.3}As/GaAs/\ Al_{0.7}Ga_{0.3}As$ heterostructure on an original and reused wafer. Insets: The 2× and 4× surface reconstruction patterns obtained by reflection high-energy electron diffraction for the original and etched substrate surfaces with and without a protection trilayer.

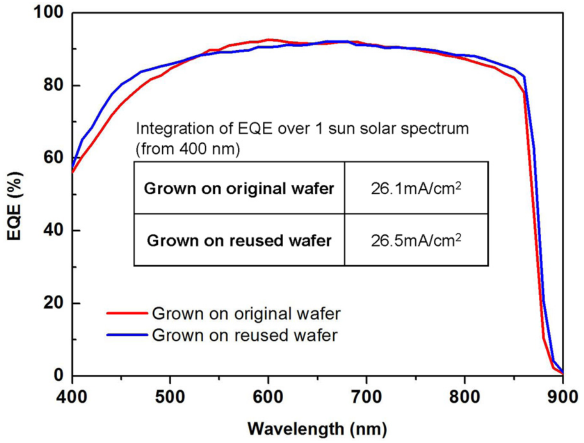

Integration of EQE over 1 sun solar spectrum (from 400 nm)

Grown on original wafer	$26.1 mA/cm^2$
Grown on reused wafer	$26.5 mA/cm^2$

FIG. 9. (Color online) EQE of photovoltaic cells grown on original and reused wafers as a function of wavelength. Inset: Short circuit current obtained by integration of the EQE spectrum over a 1 sun, AM1.5 G solar spectrum. Note that these are within experimental error of the directly measured currents in Fig. 8.

the reference. However, the RHEED patterns for the unprotected surface exhibits a spotty chevron-shaped pattern, once more indicative of a roughened surface.

Finally, solar cell epitaxial structures were grown on both the original and reused substrates, and fabricated as in Sec. II. Figure 8 shows the fourth quadrant current density versus voltage (*J-V*) characteristics of the reference and regrown photovoltaic cells measured under simulated Atmospheric Mass 1.5 Global (AM 1.5 G) illumination at 1 sun ($1\ kW/m^2$) intensity. The optical power intensity was calibrated using a National Renewable Energy Laboratory certified Si reference photovoltaic cell. The measured short circuit current and open circuit voltage, fill factor and power conversion efficiency (PCE) for both devices are nearly identical (inset, Fig. 8). In addition, the external quantum efficiencies (EQE) for the devices were measured from $\lambda = 400$ to 900 nm (Fig. 9) using a tungsten lamp, monochromator, light chopper, and lock-in amplifier. Integration of the EQE spectrum with the AM1.5 G spectrum estimates a short circuit current of $J_{sc} = 26.1\ mA/cm^2$ and $26.5\ mA/cm^2$ for GaAs solar cells grown on the original (reference) and used substrates, respectively. The discrepancy between the integrated short circuit current density and that measured directly is primarily due to absorption at wavelengths $\lambda < 400$ nm that is not accounted for in the former measurement. Additionally, slight variations of device performance possibly arise due to minor variations in fabrication from run-to-run. Finally, we note that $PCE = 23.1 \pm 0.6\%$ and $22.8 \pm 0.5\%$ for growth on the reference and used wafers, respectively.

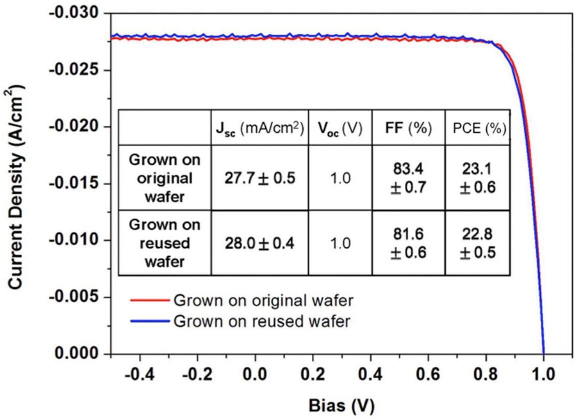

	J_{sc} (mA/cm^2)	V_{oc} (V)	FF (%)	PCE (%)
Grown on original wafer	27.7 ± 0.5	1.0	83.4 ±0.7	23.1 ±0.6
Grown on reused wafer	28.0 ± 0.4	1.0	81.6 ±0.6	22.8 ±0.5

FIG. 8. (Color online) Current density vs voltage (*J-V*) characteristics under 1 sun, AM1.5 G simulated solar illumination of the GaAs solar cells grown and fabricated on original and reused wafers using protection layers. Inset: Device performance parameters. Here, J_{sc} is the short circuit current, V_{oc} the open circuit voltage, FF the fill factor, and PCE is the power conversion efficiency.

IV. CONCLUSIONS

In summary, we demonstrated multiple, high quality epitaxial regrowths on a single GaAs wafer using a triple-layer protection scheme that was removed without damage to the original substrate surface. The substrate-growth interface for original and used wafers with and without protection layers were compared using several microscopic, morphological, and chemical probes, and indicates nearly identical quality between the original and protected wafer surfaces. Unprotected surfaces, however, show significant degradation in roughness and stoichiometric composition due to oxygen contamination during the etch process. Furthermore, the electrical and optical properties of original and regrown GaAs layers have been characterized and compared, with similar results. Finally, photovoltaic cells grown on new and reused wafers also show nearly identical performance with a PCE of approximately 23%. The high power conversion efficiencies of GaAs solar cells combined with multiple reuses of the parent wafer promise cost competitiveness with other solar cell technologies.

ACKNOWLEDGMENTS

The authors thank Mr. Yifan Zhang for assistance with photoluminescence measurements, and the Army Research Laboratory MAST program and Global Photonic Energy Corp. for partial financial support of this work.

[1] H. N. Brendan M. Kayes, Rose Twist, Sylvia G. Spruytte, Frank Reinhardt, Isik C. Kizilyalli, and Gregg S. Higashi, presented at the 37th IEEE Photovoltaic Specialists Conference, 2011.

[2] M. A. Green, K. Emery, Y. Hishikawa, and W. Warta, Prog. Photovoltaics **19**, 84 (2011).

[3] K. Lee, K. T. Shiu, J. D. Zimmerman, C. K. Renshaw, and S. R. Forrest, Appl. Phys. Lett. **97**, 101107 (2010).

[4] J. Yoon, S. Jo, I. S. Chun, I. Jung, H. S. Kim, M. Meitl, E. Menard, X. L. Li, J. J. Coleman, and U. Paik, and J. A. Rogers, Nature **465**, 329 (2010).

[5] R. Tatavarti, G. Hillier, A. Dzankovic, G. Martin, F. Tuminello, R. Navaratnarajah, G. Du, D. P. Vu, and N. Pan, in Proceedings of the Pvsc: 2008 33rd IEEE Photovoltaic Specialists Conference, Vols. 1–4, pp. 324–327 (2008).

[6] R. Tatavarti, G. Hillier, G. Martin, A. Wibowo, R. Navaratnarajah, F. Tuminello, D. Hertkorn, M. Disabb, C. Youtsey, D. McCallum, and N. Pan, in Proceedings of the 2009 34th IEEE Photovoltaic Specialists Conference, Vols. 1–3, pp. 627–629 (2009).

[7] T. Takamoto, T. Kodama, H. Yamaguchi, T. Agui, N. Takahashi, H. Washio, T. Hisamatsu, M. Kaneiwa, K. Okamoto, M. Imaizumi, and K. Kibe, Conference Record of the 2006 IEEE 4th World Conference on Photovoltaic Energy Conversion, Vols. 1 and 2, pp. 1769–1772 (2006).

[8] G. J. Bauhuis, P. Mulder, E. J. Haverkamp, J. C. C. M. Huijben, and J. J. Schermer, Sol. Energy Mater. Sol. Cells **93**, 1488 (2009).

[9] G. J. Bauhuis, J. J. Schermer, P. Mulder, M. M. A. J. Voncken, and P. K. Larsen, Sol. Energy Mater. Sol. Cells **83**, 81 (2004).

[10] Owen D. Miller, E. Yablonovitch, and Sarah R. Kurtz, e-print arXiv:1106.1603v3 (2011).

[11] G. J. Bauhuis, P. Mulder, E. J. Haverkamp, J. J. Schermer, E. Bongers, G. Oomen, W. Kostler, and G. Strobl, Prog. Photovoltaics **18**, 155 (2010).